Printed February 2, 2008

A Single Circumstellar Disk in the SVS 13 Close Binary System

Guillem Anglada[1], Luis F. Rodríguez[2], Mayra Osorio[1], José M. Torrelles[3], Robert Estalella[4,5], Maria T. Beltrán[6], Paul T. P. Ho[5,7]

ABSTRACT

We present Very Large Array observations at 7 mm of the sources IRAS 2A, IRAS 2B, MMS2, MMS3 and SVS 13, in the NGC1333 region. SVS 13 is a young close binary system whose components are separated by 65 AU in projection. Our high angular resolution observations reveal that only one of the components of the SVS 13 system (VLA 4B) is associated with detectable circumstellar dust emission. This result is in contrast with the well known case of L1551 IRS5, a binary system of two protostars separated by 45 AU, where each component is associated with a disk of dust. Both in SVS 13 and in L1551 IRS5 the emission apparently arises from compact accretion disks, smaller than those observed around single stars, but still massive enough to form planetary systems like the solar one. These observational results confirm that the formation of planets can occur in close binary systems, either in one or in both components of the system, depending on the specific angular momentum of the infalling material.

[1]Instituto de Astrofísica de Andalucía, CSIC, Camino Bajo de Huétor 24, E-18008 Granada, Spain; guillem@iaa.es, osorio@iaa.es

[2]Centro de Radioastronomía y Astrofísica, UNAM, Apartado Postal 3-72 (Xangari), 58090 Morelia, Michoacán, México; l.rodriguez@astrosmo.unam.mx

[3]Instituto de Ciencias del Espacio (CSIC)-IEEC, Gran Capità, 2, 08034 Barcelona, Spain; torrelles@ieec.fcr.es

[4]Departament d'Astronomia i Meteorologia, Universitat de Barcelona, Av. Diagonal 647, E-08028 Barcelona, Spain; robert@am.ub.es

[5]Harvard-Smithsonian Center for Astrophysics, 60 Garden Street, Cambridge, MA 02138, USA; ho@cfa.harvard.edu

[6]Osservatorio Astrofisico di Arcetri, Largo E. Fermi 5, I-50125 Firenze, Italy; mbeltran@arcetri.astro.it

[7]Academia Sinica Institute of Astronomy and Astrophysics, Taipei, Taiwan

Subject headings: ISM: jets and outflows — ISM: individual (NGC 1333, SVS 13, HH 7-11) — radio continuum: ISM — stars: formation

1. INTRODUCTION

SVS 13, in the NGC1333 region, was discovered as a 2.2 μm source by Strom, Vrba, & Strom (1976), and since the source is roughly aligned with the chain of Herbig-Haro objects 7-11 (Herbig 1974; Strom, Grasdalen, & Strom 1974), it was assumed to be the exciting source of this classical HH system. Later, Goodrich (1986) detected a faint visible counterpart of SVS 13. However, the star SVS 13 presents a number of peculiar properties. The source exhibited a significant increase of its brightness at optical ($\sim$3 mag), and IR ($\sim$1 mag) wavelengths in 1988-1990 (Eislöffel et al. 1991; Liseau, Lorenzetti, & Molinari 1992; Harvey et al. 1998), and since then, the flux has remained almost steady (Aspin & Sandell 1994; Khanzadyan et al. 2003). In addition, despite being optically visible, indicating that it is a relatively evolved young object, SVS 13 is a strong millimeter source, known as MMS1 (e.g., Grossman et al. 1987; Looney, Mundy, & Welch 2000), and presents other characteristics, such as the presence of an extremely high velocity CO outflow, that suggest it is in a much earlier evolutionary stage (a Class 0/I object; Bachiller et al. 2000).

Radio continuum emission from SVS 13 was first reported by Snell & Bally (1986). Rodríguez, Anglada, & Curiel (1997, 1999) mapped SVS 13 with the Very Large Array (VLA) at 3.6 and 6 cm (their source VLA 4). Anglada, Rodríguez, & Torrelles (2000), through VLA observations at 3.6 cm of higher angular resolution and sensitivity, discovered that SVS 13 is, in fact, a close binary system. The two components of the binary (VLA 4A and VLA 4B) are separated by $0\farcs3$, corresponding to 65 AU in projection (assuming a distance of 220 pc; Černis 1990), and have similar flux densities at 3.6 cm. The water masers associated with SVS 13 appear segregated in position and velocity, supporting the binary hypothesis (Rodríguez et al. 2002). Anglada et al. (2000) noted that the optical position for SVS 13 (as measured by Rodríguez et al. 1997) is closer to VLA 4A, while the millimeter position (Looney et al. 2000) is closer to VLA 4B. Although the precision of the astrometry available at that time did not allow an unambiguous association, this result led these authors to suggest that the strong millimeter emission reported for SVS 13 could arise from only one of the components of the binary (VLA 4B, the eastern component), while the optical emission would come from the other component (likely from VLA 4A, the western component). In the interpretation proposed by Anglada et al. (2000), only one of the stars (VLA 4B) is surrounded by a dusty envelope or disk, while the other (VLA 4A, the visible

star) is not. A similar interpretation has been proposed recently by Loinard et al. (2002) for IRAS 04368+2557 in L1527, on the basis of the morphology of the two obscured sources observed at 7 mm.

A confirmation of this interpretation for SVS 13 requires a precise comparison of the positions of the sources observed at different wavelengths, in order to identify the individual contribution of each component of the binary. Since the angular separation between VLA 4A and VLA 4B is only $0\farcs3$, absolute astrometry down to $< 0\farcs1$ is required in order to obtain an accurate enough registration of the positions. Although the accuracy of the absolute astrometry of the optical observations ($\pm 0\farcs3$) is difficult to improve due to the lack of a large enough number of suitable reference stars in the field, it is possible to improve the accuracy of the registration between the centimeter and millimeter positions by using the same instrument and calibration procedures in both wavelength ranges.

In this Letter, we present VLA observations at 7 mm of the region near SVS 13, carried out in the D and B configurations, using the same phase calibrator and procedures as in the previous VLA observations at 3.6 cm. The B configuration observations at 7 mm provide an angular resolution of $\sim 0\farcs2$, similar to that of the A configuration at 3.6 cm, and an expected accuracy in the registration between both images down to $< 0\farcs05$, allowing a precise comparison of the emission at both wavelengths, necessary to test the single disk hypothesis for the SVS 13 binary. These observations also provide 7 mm data on other sources in NGC1333: VLA 2 (MMS3), VLA 7 (IRAS 2A), VLA 10 (IRAS 2B), and VLA 17 (MMS2).

2. OBSERVATIONS

The observations were carried out at 7 mm using the VLA of the National Radio Astronomy Observatory (NRAO)[1] in the D and B configurations. The D configuration observations were carried out during 2000 September 7 using two phase centers, one near SVS 13 (at the position α(J2000) = $03^{\rm h}29^{\rm m}03\fs57$; δ(J2000) = $+31^\circ16'02\farcs8$) and a second near the source IRAS 2 (at the position α(J2000) = $03^{\rm h}28^{\rm m}56\fs14$; δ(J2000) = $+31^\circ14'31\farcs2$). For all observations an effective bandwidth of 100 MHz with two circular polarizations was employed. The absolute amplitude calibrator was 1331+305 (adopted flux density of 1.45 Jy) and the phase calibrator was 0336+323, with a bootstrapped flux density of 2.1±0.1 Jy. The data were edited and calibrated using the software package Astronomical Image Processing Sys-

[1]NRAO is a facility of the National Science Foundation operated under cooperative agreement by Associated Universities, Inc.

tem (AIPS) of NRAO. Cleaned maps were obtained using the task IMAGR of AIPS and natural weighting. The resulting synthesized beam size was $2\farcs0 \times 1\farcs6$ with P.A.$=-24°$, and we achieved an rms noise of $\sim$0.3 mJy beam^{-1}. We detected a total of five sources, whose positions, flux densities and counterparts are given in Table 1.

In order to obtain higher angular resolution data of the SVS 13 field, we carried out B configuration observations during 2001 April 20, May 4, and May 20. The array had then 23 antennas operating at 7 mm. We observed only the SVS 13 field, using the same phase center and setup as for the D configuration observations. The absolute calibrator was 1331+305 (adopted flux density of 1.45 Jy) and the phase calibrator was 0336+323, with a bootstrapped flux density of 2.8$\pm$0.3 Jy. Because of poor weather conditions on April 20 and May 20, only the May 4 data were used. Data were processed using AIPS and cleaned maps were obtained using natural weighting. The resulting synthesized beam size was $0\farcs18 \times 0\farcs16$ with P.A.$=-65°$, and we achieved an rms noise of $\sim$0.3 mJy beam^{-1}. Positions, flux densities and counterparts of the sources detected are given in Table 1.

3. DISCUSSION

We detect at 7 mm the sources VLA 2 (MMS3), VLA 7 (IRAS 2A), VLA 10 (IRAS 2B), and VLA 17 (MMS2=SVS 13B) (see Table 1). These sources were previously observed at 3.6 and 6 cm by Rodríguez et al. (1999), where a discussion on their properties and counterparts can be found. VLA 7, VLA 10, and VLA 2 were further observed at 3.6 cm with higher angular resolution by Reipurth et al. (2002). Interferometric observations at 3 mm of VLA 7 and VLA 10 have been recently reported by Jørgensen et al. (2004).

We also detect SVS 13 at 7 mm, as an unresolved source in the D configuration, and resolving it in its two components (VLA 4A and VLA 4 B) in the B configuration observation (see Table 1). In Figure 1 we compare the 3.6 cm map observed with the A configuration (Anglada et al. 2000) with the 7 mm map observed with the B configuration (this paper). Both maps were obtained with a similar angular resolution of $\sim 0\farcs2$. The positions of the sources in the two maps are in agreement within $0\farcs02$, eliminating, thus, any ambiguity in their identification at different wavelengths. As can be seen in the figure, at 3.6 cm both sources present a similar flux density, while at 7 mm VLA 4B is much stronger than VLA 4A, suggesting that VLA 4B is the dominant source in the millimeter wavelength range, with a negligible contribution from VLA 4A.

In order to quantitatively confirm this hypothesis it should be verified that the increase of flux density of VLA 4B over VLA 4A at 7 mm is caused by dust emission, and not by

free-free emission with a steep spectral index. Usually, the emission at wavelengths longer than a few cm is dominated by the free-free emission from ionized gas, while the emission at wavelengths shorter than a few mm is dominated by thermal emission from dust. Since the wavelength of 7 mm falls in between the centimeter and millimeter regimes, it should be checked, for each particular object, which is the nature of the dominant emission at this wavelength. To do that, we have plotted in Figure 2 the highest angular resolution data available on SVS 13 in the centimeter and millimeter ranges. The flux densities of VLA 4B at 3.6 cm and 1.3 cm give a spectral index of $\alpha = 1.36 \pm 0.26$, which is typical of a thermal ionized jet or a partially optically thick ionized region. An extrapolation at 7 mm of this free-free emission yields a flux density of $\sim$1 mJy, much smaller than the observed value. On the other hand, a fit to the observed data from 3.4 mm to 1.3 mm (that are supposed to trace dust emission) gives a spectral index $\alpha = 2.55 \pm 0.05$ in the millimeter range, resulting in an extrapolated flux density at 7 mm in good agreement with the value observed for VLA 4B (see Table 1 and Fig. 2). Then, we conclude that free-free emission cannot account for the observed flux density of VLA 4B at 7 mm, and that a contribution of a different nature, namely, thermal dust emission, likely from a circumstellar disk surrounding this object, is required.

In the case of VLA 4A, the overall 3.6 cm, 1.3 cm, and 7 mm data points can be fitted together with a single spectral index $\alpha = 1.25 \pm 0.20$, indicating that the observed flux density at 7 mm can be explained as free-free emission (see Fig. 2). However, we cannot discard a small contribution from dust emission at 7 mm, since an extrapolation of the 3.6 and 1.3 cm data alone gives a free-free contribution at 7 mm slightly below the observed flux density of VLA 4A. The difference ($\lesssim$0.8 mJy) could correspond to a contribution from dust, being it about five times smaller than in the case of VLA 4B.

In summary, our results indicate that of the two components of the SVS 13 binary system, the source VLA 4B is associated with a much larger amount of dust than the source VLA 4A. This strongly supports the proposal by Anglada et al. (2000), who suggested that the millimeter source MMS1 is the counterpart of the centimeter source VLA 4B. On the basis of the available optical astrometry, these authors also proposed that VLA 4A is the counterpart of the visible star SVS 13.

VLA 4B appears as a compact source in our 7 mm map obtained with the B configuration with an angular resolution of $\sim 0\farcs2$ (Fig. 1b), suggesting that the dust emission traced by this source originates in a compact circumstellar structure, likely a disk, with radius $\lesssim 30$ AU. The size of the disk is smaller than that of the typical accretion disks observed around single T Tauri stars, with radii of 100-150 AU (e.g., Dutrey et al. 1996; Wilner et al. 2000), and is more similar to that of the compact disks observed in the L1551 IRS5 binary system

(10 AU; Rodríguez et al. 1998), suggesting that they are truncated by the tidal effects of the companion star. The 7 mm flux density of VLA 4B, together with the millimeter data shown in Figure 2, can be fitted by a simple disk model. We assume a geometrically thin, vertically isothermal disk, characterized by power-law radial dependences of temperature and surface density, and we adopt the opacity law given by D'Alessio, Calvet, & Hartmann (2001). The data are fitted with a distribution of dust grains with a maximum size of 1 mm, a temperature distribution $T(r) = 470\ (r/\mathrm{AU})^{-0.5}$ K, a surface density $\Sigma(r) = 2800\ (r/\mathrm{AU})^{-1}$ g cm^{-2}, implying a disk mass of 0.06 $M_{\odot}$, for a radius of 30 AU. Thus, it seems plausible that the emission of VLA 4B is tracing a protoplanetary disk, since the mass obtained exceeds the minimum mass required to form a planetary system like the solar one ($\sim 0.01\ M_{\odot}$). Since any dust emission associated with VLA 4A is at least five times weaker than that of VLA 4B, if a disk was associated with VLA 4A, we expect its mass to be at least five times smaller than that of the disk associated with VLA 4B. We note that the flux density observed in the D configuration is larger than the total flux observed in the B configuration, indicating an additional contribution from an extended component, likely the infalling envelope. A fit to the overall spectral energy distribution, taking into account simultaneously the contributions of different components (disks+envelope), similarly to what has been done for L1551 IRS5 (Osorio et al. 2003), would be useful to better constrain the properties of each component.

Thus, the observational results obtained for SVS 13 imply that it is feasible that the development of a protoplanetary disk occurs preferentially in only one of the components of a young close binary system, with the disk absent or much less significant in the other component. In this respect, the case of the SVS 13 binary system appears to be opposite to the L1551 IRS5 case, where both components of the binary system are associated with circumstellar disks of dust of comparable characteristics (Rodríguez et al. 1998).

These results are in agreement with theoretical simulations (e.g., Bate & Bonnell 1997) that show that, depending on the mass ratio of the components and the specific angular momentum of the system, the development of circumstellar disks can occur either around a single component or around both components of the binary. According to Bate & Bonnell (1997), a circumstellar disk forms around one of the components of the binary only if the specific angular momentum of the infalling gas is greater than the specific orbital angular momentum of that component about the center of mass of the binary. Thus, if a binary system grows to its final mass mainly via the accretion of material with low specific angular momentum, the primary may have a large circumstellar disk, while the secondary is essentially naked. The systems formed by this method are expected to be binaries with separations of the order of ~ 100 AU, and they should not be developing a significant circumbinary disk. For infall with high angular momentum, both components can develop a circumstellar disk and even a circumbinary disk can be formed.

Under this simplified scheme, the low angular momentum scenario, with a disk in only one star, appears to correspond to the case of the SVS 13 binary, where the two components are separated by 65 AU in projection, and where VLA 4A would be the secondary, whereas VLA 4B (the dominant source at millimeter wavelengths) would be the primary viewed through its circumstellar disk. On the other hand, L1551 IRS5 apparently corresponds to a case of accretion of material with higher angular momentum, with both components associated with a circumstellar disk (Rodríguez et al. 1998) and probably surrounded by a circumbinary disk (Osorio et al. 2003).

In order to confirm these suggestions, it would be interesting to obtain the orbital parameters of these systems and to identify which component is the primary through accurate measurements of absolute proper motions. Relative proper motions between the two components of the L1551 IRS5 system have been obtained recently (Rodríguez et al. 2003), and accurate absolute proper motions have been measured for the T Tau Sa/Sb system (Loinard, Rodríguez & Rodríguez 2003). At present, no proper motions are available for the SVS 13 system, but these promising results obtained for other sources suggest that this goal could be attainable in a relatively near future, providing a complete test for the properties of the SVS 13 binary system.

We thank P. D'Alessio for providing us the dust opacity code, and L. Loinard and an anonymous referee for valuable comments. We thank Z. Webster for communicating us her 1.3 mm data before publication, as well as H. Ungerechts and U. Lisenfeld for discussion on the IRAM data. GA, MO and JMT acknowledge support from MCYT grant AYA2002-00376 (including FEDER funds). GA and MO acknowledge support from Junta de Andalucía. MO acknowledges support from IAU PGF and AECI. MTB and RE acknowledge support from MCYT grant AYA2002-00205. RE acknowledges support from Generalitat de Catalunya grant 2002BEAI400032. LFR acknowledges support from DGAPA and CONACyT.

REFERENCES

Anglada, G., Rodríguez, L.F., & Torrelles, J.M. 2000, ApJ, 542, L123

Aspin, C., & Sandell, G. 1994, A&A, 288, 803

Bachiller, R., Gueth, F., Guilloteau, S., Tafalla, M., & Dutrey, A. 2000, A&A, 362, L33

Bachiller, R., Guilloteau, S., Gueth, F., Tafalla, M., Dutrey, A., Codella, C., & Castets, A. 1998, A&A, 339, L49

Bate, M.R., & Bonnell, I.A. 1997, MNRAS, 285, 33

Černis, K. 1990, Ap&SS, 166, 315

D'Alessio, P., Calvet, N., & Hartmann, L. 2001, ApJ, 553, 321

Dutrey, A., Guilloteau, S., Duvert, G., Prato, L., Simon, M., Schuster, K., & Menard, F. 1996, A&A, 309, 493

Eislöffel, J., Günther, E., Hessman, F.V., Mundt, R., Poetzel, R., Carr, J.S., Beckwith, S., & Ray, T.P. 1991, ApJ, 383, L19

Goodrich, R.W. 1986, AJ, 92, 885

Grossman, E.N., Masson, C.R., Sargent, A.I., Scoville, N.Z., Scott, S., & Woody, D.P. 1987, ApJ, 320, 356

Harvey, P. M., Smith, B. J., di Francesco, J., & Colomé, C. 1998, ApJ, 499, 294

Herbig, G. H. 1974, Lick Observatory Bulletin, 658, 1

Jørgensen, J. K., Hogerheijde, M. R., van Dishoeck, E. F., Blake, G. A., & Schoeier, F. L. 2004, A&A, 413, 993

Khanzadyan, T., Smith, M. D., Davis, C. J., Gredel, R., Stanke, T., & Chrysostomou, A. 2003, MNRAS, 338, 57

Liseau, R., Lorenzetti, D., & Molinari, S. 1992, A&A, 253, 119

Loinard, L., Rodríguez, L. F., D'Alessio, P., Wilner, D. J., & Ho, P. T. P. 2002, ApJ, 581, L109

Loinard, L., Rodríguez, L. F., & Rodríguez, M. I. 2003, ApJ, 587, L47

Looney, L.W., Mundy, G.H., & Welch, W.J. 2000, ApJ, 529, 477

Osorio, M., D'Alessio, P., Muzerolle, J., Calvet, N., & Hartmann, L. 2003, ApJ, 586, 1148

Reipurth, B., Rodríguez, L. F., Anglada, G., & Bally, J. 2002, AJ, 124, 1045

Rodríguez, L.F., Anglada, G., & Curiel, S. 1997, ApJ, 480, L125

Rodríguez, L.F., Anglada, G., & Curiel, S. 1999, ApJS, 125, 427

Rodríguez, L. F., Anglada, G., Torrelles, J. M., Mendoza-Torres, J. E., Haschick, A. D., & Ho, P. T. P. 2002, A&A, 389, 572

Rodríguez, L. F., Curiel, S., Cantó, J., Loinard, L., Raga, A. C., & Torrelles, J. M. 2003, ApJ, 583, 330

Rodríguez, L.F. et al. 1998, Nature, 395, 355

Snell, R. L. & Bally, J. 1986, ApJ, 303, 683

Strom, S.E., Grasdalen, G.L., & Strom, K.M. 1974, ApJ, 191, 111

Strom, S.E., Vrba, F.J., & Strom, K.M. 1976, AJ, 81, 314

Wilner, D. J., Ho, P. T. P., Kastner, J. H., & Rodríguez, L. F. 2000, ApJ, 534, L101

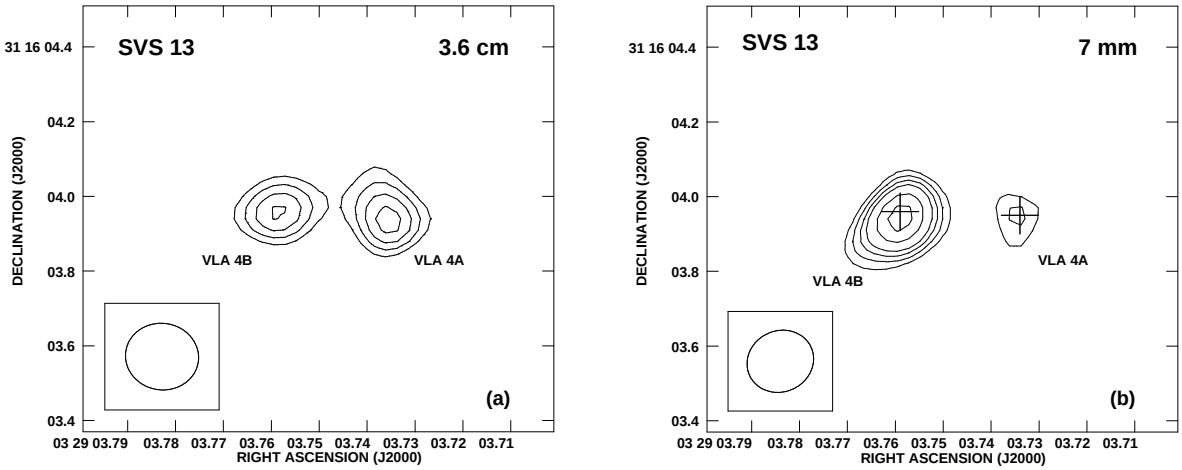

Fig. 1.— (a) VLA map (A configuration) at 3.6 cm of SVS 13, revealing that it is a binary radio source, with component VLA 4A having a similar flux density as component VLA 4B (Anglada et al. 2000). Contour levels are −3, 3, 4, 5, and 6 times the rms noise of 14 μJy beam^{-1}. (b) VLA map (B configuration) at 7 mm (this paper). Contour levels are −3, 3, 4, 5, 6, 8 and 10 times the rms noise of 0.3 mJy beam^{-1}. The crosses in this map mark the positions of the 3.6 cm sources. Note that most of the flux density at this wavelength comes from the VLA 4B component. The half power contour of the synthesized beam is shown in the lower left corner of each panel.

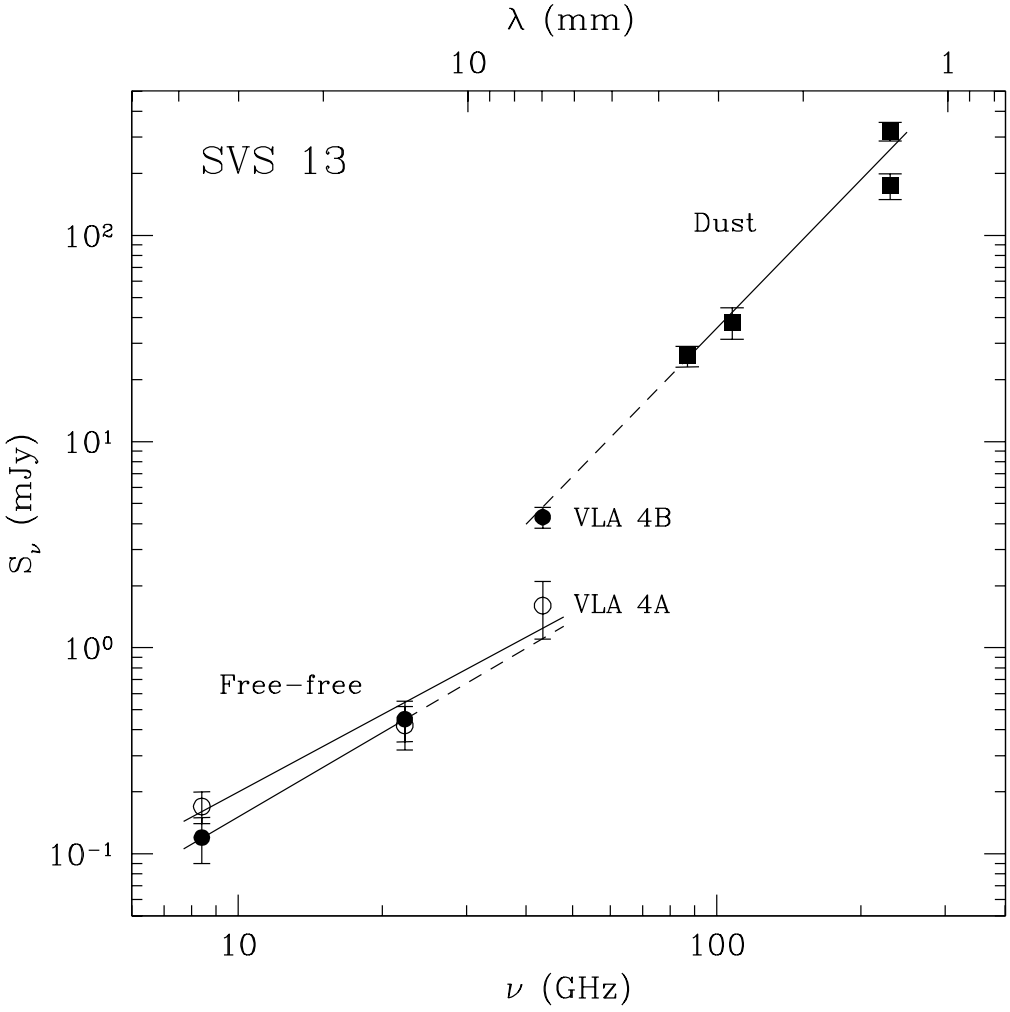

Fig. 2.— Spectrum of SVS 13 in the 3.6 cm to 1.3 mm wavelength range from data of good angular resolution. Observed flux densities of component VLA 4A (empty circles), VLA 4B (filled circles), and of the overall system (filled squares) are represented. Solid lines represent least-square fits to the data points in a given wavelength range, while dashed lines represent an extrapolation to other wavelengths. Note that the observed flux density of VLA 4B at 7 mm is in agreement with the extrapolation of the fit obtained from the 3.4 to 1.3 mm data (that are supposed to trace the dust emission), while the flux density of VLA 4A at 7 mm fits the free-free emission. Data points are from VLA observations at 3.6 cm (beam $\simeq 0\farcs2$; Anglada et al. 2000), 1.3 cm (beam $\simeq 0\farcs1$; G. Anglada et al., in preparation) and 7 mm (beam $\simeq 0\farcs2$; this paper), Plateau de Bure observations at 3.4 mm and 1.3 mm (beams $\simeq 3\farcs5$ and $1\farcs5$; Bachiller et al. 1998), and BIMA observations at 2.7 mm (beam $\simeq 0\farcs6$; Looney et al. 2000) and 1.3 mm (beam $\simeq 0\farcs3$; Z. Webster et al., in preparation).

Table 1. 7 mm Continuum Sources

Source	Position[a]		S_ν(D config)[b]	S_ν(B config)[c]	Counterpart[d]
	α(J2000)	δ(J2000)	(mJy)	(mJy)	
VLA 7	03 28 55.56	+31 14 37.1	10.0±0.5	···	IRAS 2A
VLA 10	03 28 57.37	+31 14 15.9	5.2±0.3	···	IRAS 2B
VLA 2	03 29 01.962	+31 15 38.15	9.0±1.0	10.3±1.2	MMS3
VLA 17	03 29 03.072	+31 15 51.86	8.5±0.5	6.6±0.6	MMS2 (SVS 13B)
VLA 4A	03 29 03.735	+31 16 03.95	10.8±0.6[e]	1.6±0.5	SVS 13
VLA 4B	03 29 03.759	+31 16 03.94	10.8±0.6[e]	4.3±0.5	MMS1

[a]Units of right ascension are hours, minutes, and seconds, and units of declination are degrees, arcminutes, and arcseconds. Positions given are from the B configuration data (absolute positional error is estimated to be $0\farcs05$), except for VLA 7 and VLA 10, that are from the D configuration data (absolute positional error is estimated to be $0\farcs2$).

[b]Flux density from the D configuration data.

[c]Flux density from the B configuration data.

[d]See Rodríguez et al. 1999 and references therein for a discussion on the sources VLA 7, VLA 10, VLA 2, and VLA 17 and their counterparts. See text for a discussion on VLA 4A and VLA 4B

[e]Total flux density of VLA 4A+VLA 4B. The angular resolution in this configuration cannot separate the emission of each component, although VLA 4B is likely the dominant one.